ASPIRE Flight Mechanics Modeling and Post Flight Analysis

Soumyo Dutta,[*] Eric M. Queen,[†]Angela L. Bowes,[*]

NASA Langley Research Center, Hampton, VA 23681, USA

Emily A. Leylek[‡] and Mark C. Ivanov[§]

Jet Propulsion Laboratory, California Institute of Technology, Pasadena, CA 91109, USA

The Advanced Supersonic Parachute Inflation Research and Experiment (ASPIRE) is a series of sounding rocket flights aimed at understanding the dynamics of supersonic parachutes that are used for Mars robotic applications. SR01 was the first sounding rocket flight of ASPIRE that occurred off the coast of Wallops Island, VA on Oct. 4, 2017 and showed the successful deployment and inflation of a Mars Science Laboratory built-to-print parachute in flight conditions similar to the 2012 Mars Science Laboratory (MSL) mission. SR02 was the second sounding rocket flight that also occurred off the coast of Wallops Island on March 31, 2018 and showcased the successful deployment and inflation of a new strengthened parachute being considered for the Mars 2020 mission at fifty percent higher dynamic pressure than observed on MSL. Prior to both flights, a multi-body flight dynamics simulation was developed to predict the parachute dynamics and was used, in conjunction with other tools, to target Mars-relevant flight conditions. After each flight, the reconstructed trajectory was used to validate the pre-flight dynamics simulation and recommend changes to improve predictions for future flights planned for the ASPIRE program. This paper describes the flight mechanics simulation and the post flight reconciliation process used to validate the flight models.

I.   Introduction

In the early morning of October 4, 2017, the first flight in a series of sounding rockets tests to study the dynamics of supersonic parachutes took place off the coast of Virginia near NASA Wallops Flight Facility (WFF). The test demonstrated a successful deployment, inflation, and deceleration by a supersonic parachute at Mars relevant conditions. The sounding rocket tests are a part of the Advanced Supersonic Parachute Inflation Research and Experiment (ASPIRE) program that was started in 2016 to understand the inflation and peak load performance of supersonic parachutes used for NASA's Mars robotic missions. The program's predecessor, the Low Density Supersonic Decelerator (LDSD) program, conducted two flight tests off the coast of Hawaii in 2014 and 2015 with Ringsail parachutes at inflation Mach number greater than 2.0. Both flight tests suffered failure in the parachute during the inflation process and raised questions about the understanding of parachute inflation and dynamics at Mars relevant conditions.

The ASPIRE program hopes to answer the questions raised by the LDSD program by testing the successful Mars Science Laboratory (MSL) parachute that opened and performed nominally on Mars in 2012 (see Fig. 1). The MSL/ASPIRE parachutes are Disk Gap Band (DGB) style parachutes, which differ from the Ringsail types used for LDSD, and the ASPIRE parachutes are 21.5 m in diameter, as opposed to the 30 m diameter parachutes for LDSD. The ASPIRE program hopes to test the MSL-heritage DGB and a strengthened version of the parachute at conditions close to the MSL parachute experience at Mars and

---

American Institute of Aeronautics and Astronautics

then at higher inflation conditions to build margin against the flight limit load. It is hoped that a successful completion of the test matrix by these ASPIRE DGB parachutes will restore faith in the inflation modeling of supersonic parachutes at Mars conditions that were put into doubt due to the parachute failures experienced by LDSD.[1] Ultimately, the tested parachutes will inform the design of the parachute flown by MSL's follow-on mission, Mars 2020, which plans to use a 21.5 m DGB parachute when it lands on Mars in 2021.
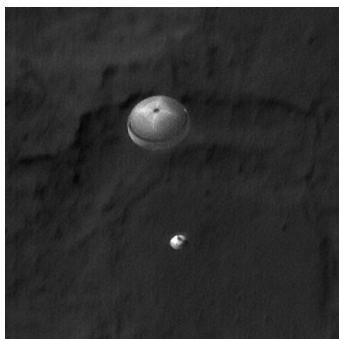
Since the flight of SR01 in October 2017, the ASPIRE program has also successfully demonstrated the first flight of the strengthened parachute on March 31, 2018 during the SR02 test. This paper will provide an introduction to the ASPIRE flight project, its concept of operations, and discuss the flight mechanics models that were used for pre-flight predictions, targeting, and operations. Finally, the simulation results will be compared with the post flight reconstructed performance of ASPIRE SR01 and SR02.

Figure 1. Mars Science Laboratory's Disk Gap Band (DGB) parachute and descent stage. (Image Credit: NASA/JPL-Caltech/University of Arizona)

II. ASPIRE Flight Project

The ASPIRE flight concept of operations is shown in Fig 2. The test vehicle and parachutes are launched on-board NASA's Sounding Rocket Operations Contract (NSROC) sounding rockets. For ASPIRE, the sounding rocket stack (as shown in Fig. 3) consists of a Terrier first stage, a Black Brant second stage, and a 1200 kg test vehicle that includes the parachute system comprising the payload. The sounding rocket stack is launched and initially spin stabilized at approximately 3 Hz. The first and second stage burnout occurs at 5 and 35 s respectively after launch and the payload section separates from the second stage at 104 s. At payload separation, the vehicle nominally is around Mach 1.2 and at 50 km altitude. The test vehicle nominally reaches apogee around 51 km after which the vehicle begins accelerating as it descends. MSL was at Mach 1.7 and a dynamic pressure of 474 Pa when the parachute was fully deployed on Mars.[2] For ASPIRE SR01, the on-board flight software triggers mortar fire to begin at a value so that at parachute full inflation the vehicle attains Mars like deployment conditions. For SR02, the target was approximately 50% higher than MSL flight conditions; thus, the target full inflation dynamic pressure was 678 Pa while the target Mach number at full inflation was still close to Mach 1.7. After the parachute inflates, the vehicle decelerates rapidly to subsonic conditions and finally splashes down in the Atlantic Ocean approximately 60 km East from WFF. Shortly before splashdown, the vehicle ejects the heavily weighted nosecone to improve the buoyancy of the rest of the payload. The nosecone has ballast to improve the conditions that can be achieved at parachute deployment.

The test vehicle can be seen in Fig. 3. The payload is 6.66 m in length and 0.72 m diameter at its largest cross-section. The front portion of the vehicle consists of the ballast and buoyancy foam, while the back end consists of mortar and other parachute deployment systems. The middle section of the payload consists of the Gimbaled LN-200 Miniature Flight Computer (GLN-MAC) that is used for triggering events, such as mortar fire, and the NSROC Inertial Attitude Control System (NIACS). The test vehicle is spin stabilized during launch leading up to payload separation and actively controlled by the NIACS from separation to mortar fire. In early analysis, it was discovered that active attitude control is needed to maintain the vehicle at the desired attitude for parachute deployment. The NIACS is turned off at mortar fire to allow the dynamics of the parachute and its effect on the test vehicle to be observed without any external moments.

The test article for ASPIRE SR01 was the MSL heritage DGB parachute. The dimensions of the various components of the final test configuration are shown in Fig. 4. The final constructed diameter of the parachute for ASPIRE SR01 was 21.35 m and the projected diameter was 15.7 m. For SR02, the test article was a strengthened DGB parachute designed for the Mars 2020 mission.[1] The dimensions of the parachute were similar to the SR01 article, although the mass of the parachute was higher due to the use of strengthened fabrics and the mortar force was higher to compensate for the heavier parachute. Ref. 1 discusses the difference between the SR01 and SR02 parachutes. For both ASPIRE flights, the test vehicle is attached to the parachute canopy through various Kevlar lines. The three lines directly attached to the back end of the test vehicle are the bridle lines, which come together at a triple bridle confluence point (TBCP). The riser line is also attached to the TBCP and that line in turn is connected to the canopy via suspension lines. These lines provide a variety of stiffness and damping between the parachute canopy and the rigid

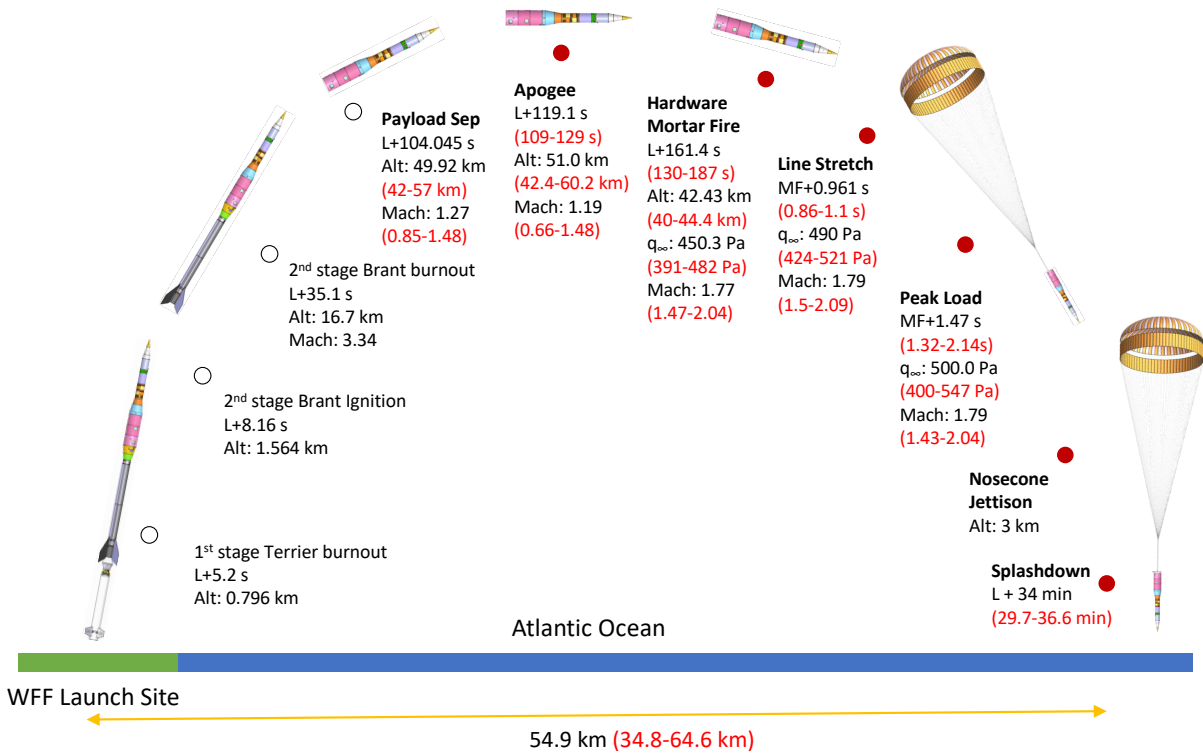American Institute of Aeronautics and Astronautics

Figure 2. ASPIRE concept of operations. Reconstructed values in black and pre-flight min/max predictions are in red are for SR01 flight. SR02 flight conditions are listed in the results section of the paper.
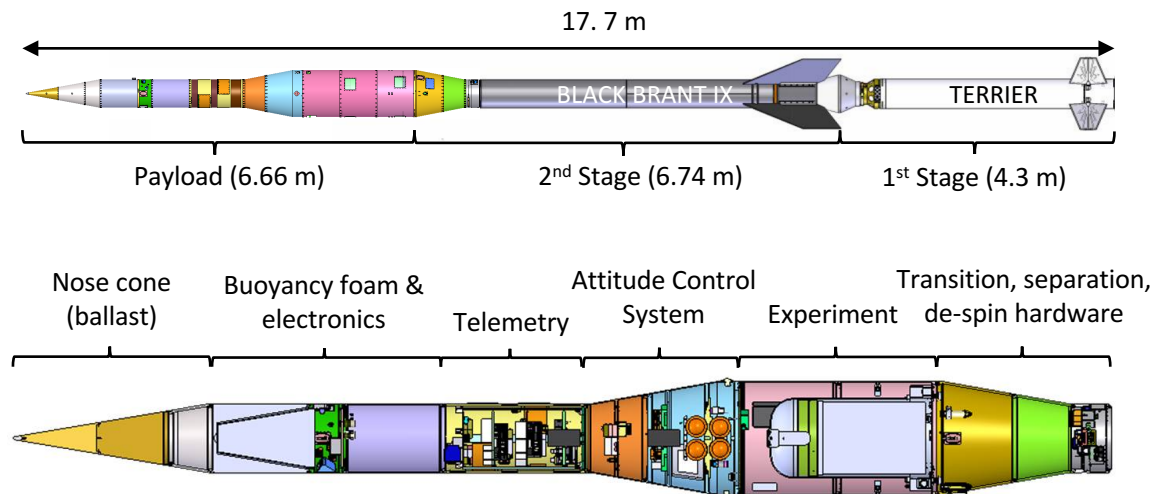

Figure 3. ASPIRE flight vehicle configuration.

American Institute of Aeronautics and Astronautics

test vehicle. The next section will discuss how this multi-body system was modeled in the flight mechanics simulations to provide pre-flight performance predictions.
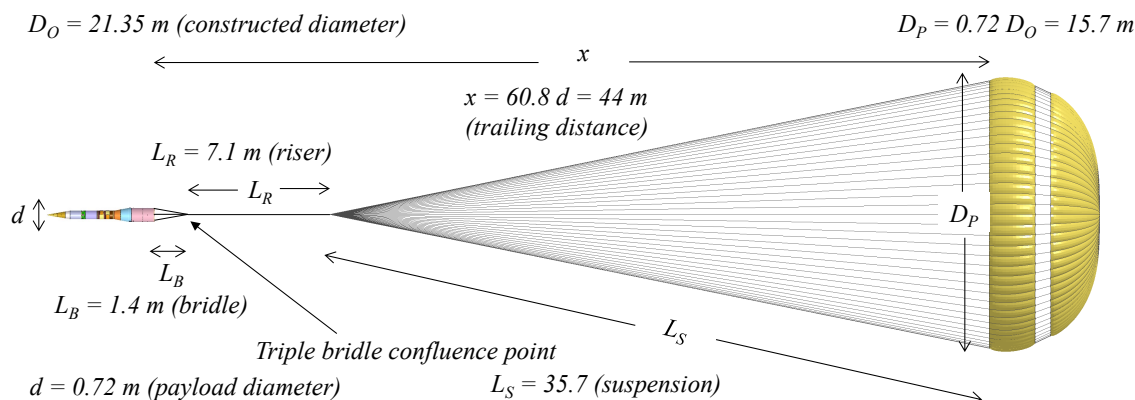

Figure 4. ASPIRE test vehicle and SR01 parachute system. The dimensions of the SR02 parachute were similar although the fabric strengths were higher.

III.   Simulation Detail

Pre-flight prediction of the vehicle's performance and targeting of the mortar fire trigger to hit desired parachute performance were achieved via flight mechanics simulations that modeled various aspects of the flight profile from launch to splashdown. The powered portion of the flight profile was handled by WFF's tools, while the test portion of the flight, from ASPIRE separation to splashdown, were modeled by two other flight mechanics simulations. These two flight mechanics simulations – NASA Langley Research Center's Program to Optimize Simulated Trajectories II (POST2) and NASA Jet Propulsion Laboratory's Dynamics Simulator for Entry, Descent, and Surface Landing (DSENDS) – were used in concurrence to develop flight parameters and inform stakeholders while providing verification and validation to each other during the development. There are subtle differences between the two simulations; however, in this paper the focus is on the POST2-based simulation that provided multi-body predictions for the ASPIRE SR01 and SR02 flights. The reader is referred to Refs. 3-4 for information about DSENDS simulations for similar flight mechanics problems.

POST2 has been the tool to model flight mechanics for many previous flight missions. POST2 is a six degree-of-freedom flight dynamics simulation tool that can simultaneously simulate the trajectory of up to 20 independent or connected rigid bodies. It is a generalized point mass, discrete-parameter targeting and optimization trajectory simulation program with multi-vehicle capabilities that integrates translational and rotational equations of motion along the trajectory. The simulation tool has significant entry, descent, and landing (EDL) flight heritage as it has been used in the past successfully for several Mars EDL missions, such as Mars Pathfinder,[5] Mars Exploration Rovers,[6] Mars Phoenix,[7] and Mars Science Laboratory.[8] Additionally, the POST2 was also used on LDSD's flights 1[9–11] and 2.[12, 13]

The ASPIRE simulation is based on the POST2 simulations used in LDSD to model the multi-body dynamics of the flight article. The simulation incorporates various engineering models for the vehicle and the environment. These models include vehicle mass properties, mortar fire orientations, computational fluid dynamics (CFD)-based aerodynamic predictions of the test vehicle during flight, parachute aerodynamics based on wind tunnel tests, flight software used for triggering during flight, model of the NIACS, and atmospheric property predictions initially from Earth Global Reference Atmospheric Model (Earth-GRAM 2010)[14] and later from NASA's Goddard Earth Observing System model version 5 (GEOS-5).[15] The models and their uncertainties are varied in Monte Carlo fashion to provide statistical estimates of various flight performance parameters, such as trajectory conditions at parachute full inflation and splashdown predictions.

In the next few sections, some of the key modeling aspects of the simulation are discussed.

A. Multi-Body Dynamics

The POST2 multi-body dynamics model is based on simulating the response between two rigid, six degree of freedom (DOF) vehicles connected by lines. For ASPIRE, the two 6DOF rigid bodies are the test vehicle and the parachute, which are connected by tension-only bridle lines that have stiffness and damping. Treating the parachute as a rigid vehicle is a key assumption as it is modeled as a single vehicle from the TBCP up to the canopy with mass properties that include the mass of the canopy, suspension lines, and riser lines. Of course, in reality, the parachute is a flexible body while the suspension lines and riser line also have their own mass, stiffness, and damping. However, multi-body simulations used for other flight projects in the past have shown that modeling the parachute down to the TBCP as a rigid body and then connecting that body to the forebody via tension-only bridle lines provides attitude and force response that is comparable to flight data.[2] Thus, for ASPIRE, the same assumptions were made.

The multi-body phase of the modeling starts at mortar fire, when a test vehicle ejects the parachute bag using the mortar engine. The mortar is modeled as a thruster that applies a constant force on both the parachute bag vehicle and the test vehicle for a finite time. The mortar thrust direction can be varied based on alignment uncertainty for Monte Carlo analysis. The parachute bag, which is a 3DOF vehicle, is pushed along the length of the parachute can until it fully exits from the separation plane of the test vehicle. While the bag is in the parachute can, a constraint force equations (CFE) based model[16] is used to constrain the motion of the bag axially and also simulate the friction on the bag. The initial phase of the multi-body dynamics is shown in Fig. 5(a).
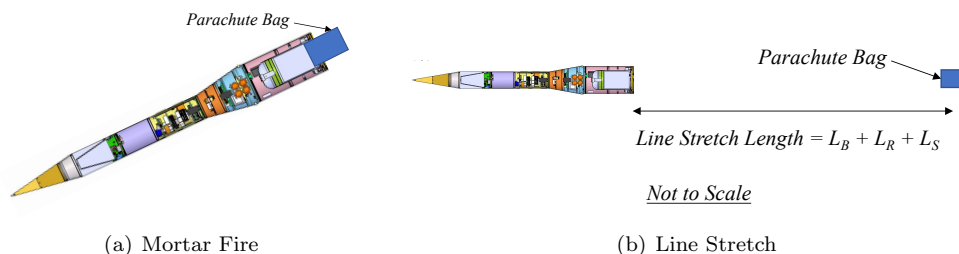

Parachute Bag

Parachute Bag

Line Stretch Length = $L_B + L_R + L_S$

Not to Scale

(a) Mortar Fire   (b) Line Stretch

Figure 5. Multi-body model dynamics for ASPIRE.

After the parachute bag exits the test vehicle, the only force acting on this vehicle are gravity. Although in reality the bag experiences aerodynamic drag, this force model is very difficult to model with CFD tools especially since the bag is in the unsteady wake of the test vehicle. Assuming no drag provides a conservative estimate of the time to the line stretch event.

Upon reaching the line stretch distance, shown in Fig. 5(b), the parachute bag vehicle is replaced by the 6DOF rigid parachute body. The line stretch distance is the sum of bridle lines length (L_B), riser line length (L_R), and suspension lines length (L_S). Recall, the parachute vehicle starts at the TBCP, where the three bridle lines provide the connection to the test vehicle via tension-only lines. The stiffness and damping of the tension lines are based on Kevlar line properties of the actual bridle lines. The attitude of the parachute vehicle cannot transfer from the parachute bag vehicle which is modeled as a 3DOF vehicle. Instead, the parachute bag is initialized at a prescribed angle relative to the payload that is varied in a Monte Carlo simulation. This angle is empirically informed by previous flight data and wind tunnel tests. However, most DGB test data consist of a blunt body forebody similar to entry aeroshells. Blunt bodies have larger wakes than the relatively slender body of the ASPIRE test vehicle. Thus, the parachute initialization angle choice for ASPIRE was a mixture of previous data and engineering judgment. The ASPIRE SR01 and SR02 flight data and the ensuing reconstruction will inform the initial parachute angle for future ASPIRE flights.

Once the line stretch condition has been achieved and the parachute vehicle has been initialized, the two rigid bodies behave under their separate aerodynamics albeit responding to each other due to forces from the lines connecting them. The test vehicle aerodynamics is discussed by Van Norman et. al.,[17] while the ASPIRE parachute aerodynamics is discussed by Muppidi et. al.[18] and O'Farrell et. al.[19] However, some mention of the parachute aerodynamics is necessary to describe the multi-body model. The parachute aerodynamics consists of 6DOF aerodynamic coefficients, such as tangential force, normal force, and pitching coefficient moment, and the vehicle is treated as an axisymmetric body. The aerodynamics are a function of Mach number and angle of attack. During inflation, the parachute aerodynamic force changes from zero

at line stretch to peak load at full inflation based on power law dependent on time since line stretch and time to full inflation.[20] The inflation time itself is based on the distance it takes for the parachute to travel a fixed inflation distance[21] which is determined empirically and varied in Monte Carlo analysis.

After the full inflation time has elapsed, the configuration in the simulation looks similar to what is shown in Fig. 4. At full inflation, other models are turned on in the simulation. The parachute has inflated by capturing a volume of atmosphere. This captured atmosphere adds to the parachute mass as so-called apparent mass. The captured atmosphere also provides a buoyant force to the vehicle. These forces are activated at full inflation since their effects are captured during the inflation process by the value of opening load factor that is applied to the aerodynamic force. Additionally, while the parachute vehicle is above Mach 1.4, it experiences areal oscillation, where the force of the vehicle fluctuates based on a random process that simulates the collapse and re-inflation of the canopy observed during the deployment of supersonic parachutes in the past. Cruz et. al. discuss the parachute model in great detail in Ref. 20, while Way describes the inflation dynamics in Ref. 22. These models will be evaluated post flight with reconstructed trajectory information.

B. Flight Software and NIACS Modeling

Active attitude control between ASPIRE separation and mortar fire was necessary to maintain desired attitude at parachute deploy. Thus, a high fidelity model of the NIACS firings was integrated with the simulation. The flight software was integrated into LDSD flight mechanics simulations in the past as well.[9, 12]

For ASPIRE, the flight software that provides the NIACS commands requires position, velocity, attitude, and attitude history. Additionally, polynomials representing the atmospheric density and the East/West and North/South winds at various altitudes are loaded into the flight software to provide prediction of the the dynamic pressure of the vehicle based on the navigated filter states. Using the estimated dynamic pressure, the flight software provides a signal to the mortar to fire when the target dynamic pressure is reached. This is the software trigger for the mortar fire to start, while the actual mortar fires after a short lag at a time called hardware mortar fire. Moreover, the flight software also provides the NIACS command necessary to maintain desired attitude and rates using roll, pitch, and yaw control thrusters between separation from booster and software mortar fire.

The NIACS cold gas actuators that are modeled in the simulation are fired based on the commanded values from the flight software. The NIACS actuators consist of four roll thrusters (two for counter-clockwise control and two for clockwise control), four thrusters for pitch and yaw control at a low level, and four additional thrusters for pitch and yaw control at a higher (or super) level. A delay between the NIACS command and the actuator action is modeled to match previously observed delay in NIACS flight data. Moreover, when multiple thrusters are firing, there is a decrement in thrust due to total pressure drop in the lines, which is also captured in the actuator model.

Models such as the NIACS and the multi-body dynamics allows the flight mechanics simulation to create predictions for various phases of flight. Of special interest are states at mortar fire, where the parachute deployment event is triggered, and full inflation, where Mars-relevant conditions are to be met as part of experimental objectives for ASPIRE. In subsequent sections, these pre-flight predictions are compared with the reconstructed values from the ASPIRE SR01 and SR02 trajectories.

C. Operations Support

A key requirement of the ASPIRE simulations was to provide day-of-flight and operations support. This was conducted by gathering forecast atmospheric profiles, creating polynomials that represented these forecast atmospheric profiles for the flight software, and then using these polynomials in simulation to determine the target dynamic pressure. During analysis done before SR01, it was found that the daily shift in atmospheric properties, such as winds, affected both the splashdown prediction of the test vehicle appreciably and changed the target conditions needed to hit the MSL-like flight conditions. Thus, a system was created for SR01 where the forecast GEOS5[15] atmosphere for the day-of-launch and time of launch would be downloaded at multiple times one day before launch (L-1 predictions). Using the L-1 prediction 24 hours before the flight for the targeted flight time (8 am), the flight constants such as the atmospheric polynomials and the target conditions were generated and passed on to the flight operations team. The flight performance was be monitored with updated Monte Carlo simulations that used more recent atmospheric predictions to understand if the changing atmospheric conditions were moving the flight vehicle outside the bounds of

American Institute of Aeronautics and Astronautics

requirements. Then on the day of launch, splashdown predictions were provided with the latest atmospheric predictions; these splashdown predictions were passed on to the recovery team that wanted to recover the parachute, the payload, and the on-board data shortly after the test vehicle splashed into the water.

SR02 had similar requirements; however, a recovery zone estimate was also made two days before the launch (L-2) to meet range safety requirements. Additionally, on the actual day of flight, SR02 flew at 12:19 pm instead of the usual target of launch around 7:30-8:00 am due to concerns regarding the sea states. This was different than SR01 where the flight flew at 7:30 am and the on-board polynomials were targeted for a launch at 8 am. The change in launch time for SR02 meant that the flight targets were tuned for a different launch time than when the vehicle actually flew. So the difference in the flight performance were tracked with several other Monte Carlos that had updated GEOS5 forecasts for various launch times.

IV.   Flight Mechanics Predictions and Reconciliation with Flight Data

ASPIRE SR01 and SR02 had many different instruments on-board to assist post flight reconstruction of the trajectory.[19] Part of the NIACS package is an inertial measurement unit (IMU) called the gimbaled LN-200 with miniature airborne computer (GLN-MAC) that records the acceleration and angular rates sensed on-board the test vehicle at a rate of 400 Hz. The test vehicle is also equipped with a GPS receiver that provides updated position and velocity states. The vehicle was tracked using an on-board C-Band transponder and by skin tracking from three WFF radars. The ASPIRE vehicle also has a pair of situational GoPro cameras and another pair of high resolution, high speed cameras that provided good videos of the inflation process. Moreover, multiple high altitude balloons with radiosondes captured atmospheric profile data up to 40 km altitude on the day of launch.

The IMU, GPS, radar, and balloon data were used within an Extended Kalman Filter (EKF) based tool, called New Statistical Estimation Program (NewSTEP), to provide post flight best estimated trajectory (BET).[23] In the following sections, ASPIRE SR01 and SR02 reconstructed trajectory are compared with pre-flight Monte Carlo estimates. In most instances, the reconstructed flight conditions fall well within the pre-flight Monte Carlo distributions that provided statistical estimates of conditions at major events of interest. However, in cases where the pre-flight estimates fail to match the reconstruction, the process of reconciliation is undertaken to adjust the pre-flight models to understand what components of the simulation should be modified to better capture the mechanics of reality. The process of reconciliation was used after the two LDSD flights[11, 13] with great result, and led to new model designs that improved the pre-flight estimate of the ensuing flights, including the two ASPIRE flights. The same reconciliation process is followed here to inform the model changes for future ASPIRE flights.

A.   ASPIRE SR01 Reconstruction and Reconciliation

Fig. 6 shows the comparison of the pre-flight predictions in the form of histograms versus the post flight BET value shown as vertical lines. The pre-flight predictions are a result of Monte Carlo analysis where various simulation settings, like atmosphere, aerodynamics, mass properties were dispersed randomly for 2000 cases to aggregate statistics about events of interest. The reconstructed BET values are listed as percentiles of the Monte Carlo result, where a low (close to 1) or high (close to 100) percentile denotes that the reconstruction is a low probability event while a percentile close to 50 denotes that the value is close to the median of the prediction and is thus a high probability event. In general, as one approaches the tails of a Monte Carlo distribution, the probability decreases greatly, and so a small percentile difference in the tails of a distribution corresponds with a large probability difference of that event according to the distribution.

Looking at the trajectory states at events through mortar fire, the flight mechanics simulation's pre-flight predictions seem to match very well with the reconstructed BET. Reconstructed Mach number, total angle of attack, and altitude all seem to be within a high confidence area of the pre-flight prediction. The dynamic pressure at mortar fire is at a lower probability (92nd percentile) within the pre-flight estimates, but since the Mach number is not a low probability event, it suggests that there is difference between the pre-flight estimate of atmospheric density and that was seen in flight.

Comparing predictions with BET at full inflation and splashdown events, as shown in Fig. 7, show good agreement between the simulation and the reconstruction. Dynamic pressure at full inflation from the BET is at lower probability most likely due to the difference in pre-flight and actual density. However, the BET Mach number, pull angle at full inflation, and splashdown time appear to be high probability events in the
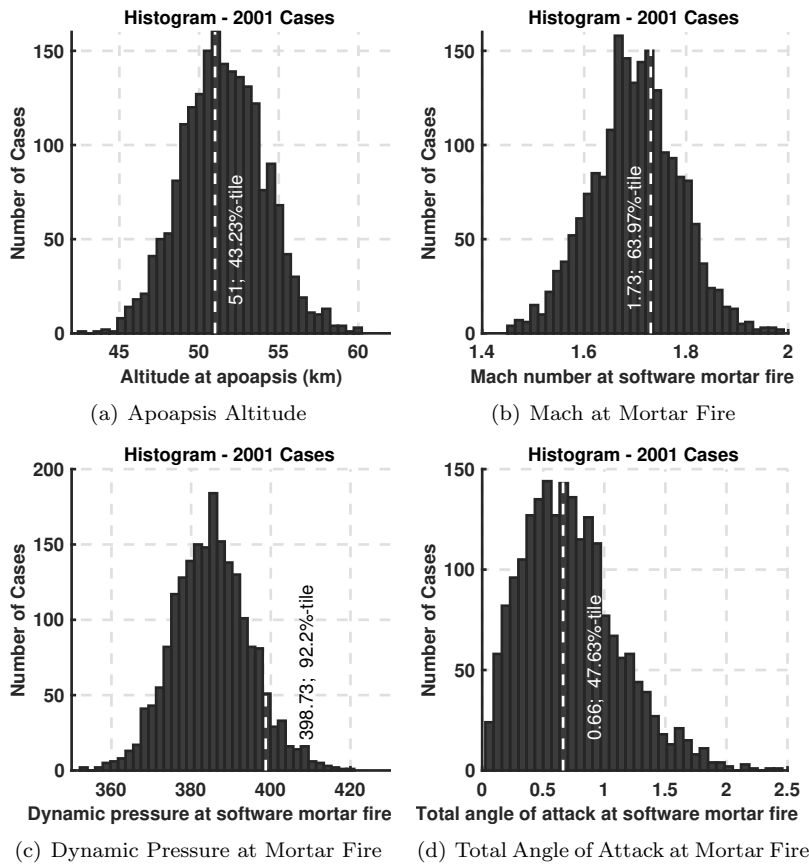
(a) Apoapsis Altitude   (b) Mach at Mortar Fire

(c) Dynamic Pressure at Mortar Fire   (d) Total Angle of Attack at Mortar Fire

Figure 6. Pre-flight Monte Carlo predictions (histograms) and comparison to reconstruction (white line) through mortar fire for ASPIRE SR01.

pre-flight predictions.

ASPIRE SR01 flight was very close to nominal and did not have many events that were very low probability events in the pre-flight Monte Carlo. The exception was the dynamic pressures at mortar fire and full inflation. Thus, for reconciliation, two pre-flight Monte Carlo settings were adjusted that were not known apriori to compare simulation results with reconstruction. The atmosphere used in the pre-flight simulations were GEOS5 forecasts. Post flight, the reconstructed atmosphere[23] was available for use in the Monte Carlo. Additionally, post flight the exact state of the vehicle at separation (the initial condition of the simulation) was known due to flight navigation states. When these two model settings were adjusted in the simulation, the new predictions, as shown in Fig. 8, become more in line with the reconstructed states, even for previously low probability events such as dynamic pressure at mortar fire.

Another change incorporated within the final reconciled Monte Carlo is a change in the distribution of a parameter that controls the inflation time.[21] For SR01, there was scant data to predict the inflation time of a supersonic parachute in the wake of a slender body. So based on DGB data from previous flights where the payload had been blunt bodies, a rather large dispersion of inflation time was selected for SR01. However, post SR01, the inflation model was adjusted to match flight data and the dispersion was reduced. This updated inflation model was used in Fig. 8(d) and led to a closer match in inflation time in the reconciled simulation than the pre-flight prediction.

The nominal case for the final reconciliation Monte Carlo – with updated atmosphere and separation states – also compares well with the NIACS flight command history recorded on-board. Fig. 9 shows the firing command history from the flight and its equivalent from the nominal case of the reconciled Monte Carlo. In the figure, 1 or -1 means a thruster is on and 0 means a thruster is shut-off. Although the thruster firings are not identical between the flight data and the simulation, on a macroscopic level the firing histories line up in time. The comparison of the integrated NIACS firing time from the flight data and simulation in Table 1 is not show an exact match; however, the differences are not unreasonable considering one is
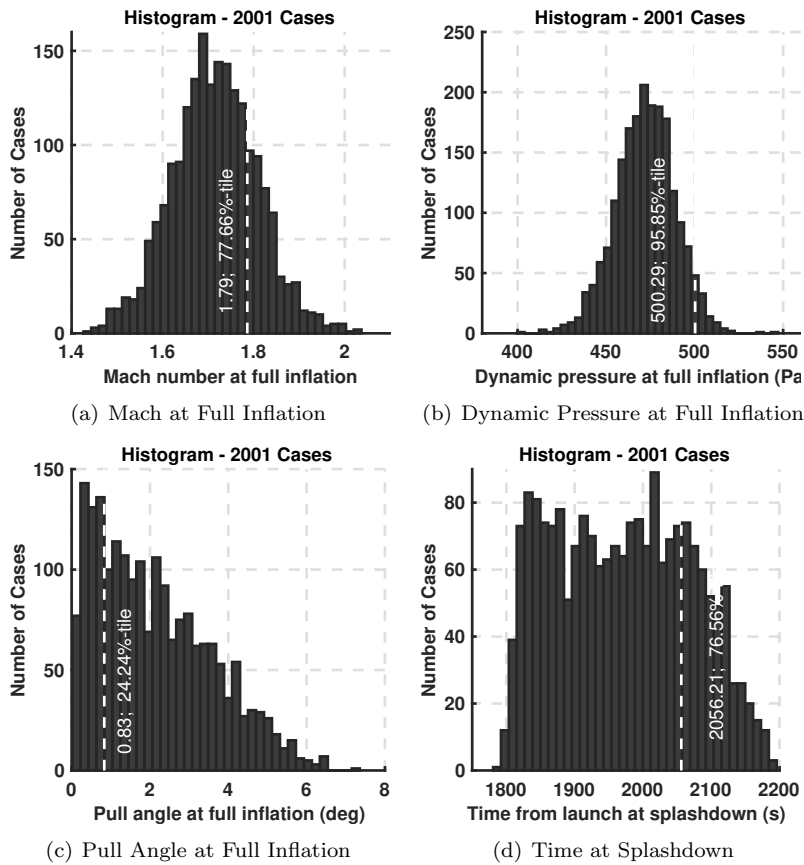
American Institute of Aeronautics and Astronautics

(a) Mach at Full Inflation

(b) Dynamic Pressure at Full Inflation

(c) Pull Angle at Full Inflation

(d) Time at Splashdown

Figure 7. Pre-flight Monte Carlo Predictions (histograms) and comparison to Reconstruction (white line) through Splashdown for ASPIRE SR01.

comparing a single Monte Carlo case to the flight data and the integrated times show that the NIACS in flight behaved similarly to the NIACS modeled in the simulation over the course of the 60 s long coast phase.

Table 1. NIACS Integrated Firing Timing for ASPIRE SR01.

Thruster Name	Flight Data (s)	Reconciliation (s)
v0	0.760	1.390
v90	1.000	1.020
v180	1.620	1.970
v270	0.100	0.540
vcw	0.180	0.210
vccw	1.720	1.850
vsuper	1.220	0.800

Some of the trajectory states from the reconciliation Monte Carlo nominal are co-plotted with the BET profile in Fig. 10. The focus here is during the experiment part of the flight, which includes the coast phase and the parachute deployment phase (100 s to 200 s after launch). One can see that once atmosphere and separation states are adjusted in the simulation to match the day of flight data, the reconciliation simulation is comparable to the BET states.

The ground tracks are compared in Fig. 11, where the pre-flight prediction used for recovery and the reconciliation Monte Carlo nominal are co-plotted with the BET profile. Both the pre-flight and reconciliation simulation trajectories are within 0.5 nautical miles of the GPS splashdown location, demonstrating the nominal nature of the SR01 flight.
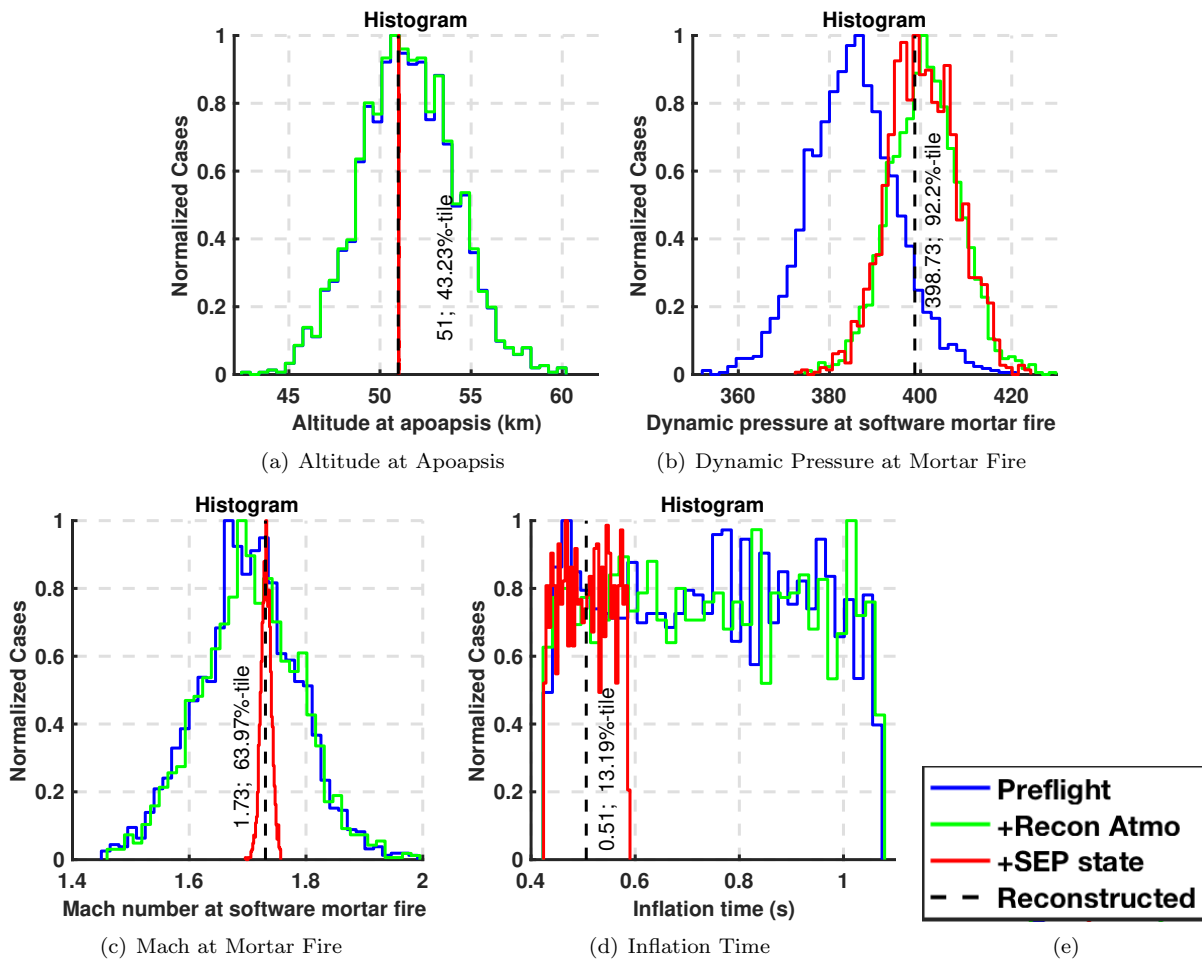
American Institute of Aeronautics and Astronautics

(a) Altitude at Apoapsis   (b) Dynamic Pressure at Mortar Fire

(c) Mach at Mortar Fire   (d) Inflation Time   (e)

Figure 8. Reconciliation results for ASPIRE SR01. Reconstruction line in black shows the percentile compared to the pre-flight prediction.

B. ASPIRE SR02 Reconstruction and Reconciliation

Fig. 12 shows the comparison for ASPIRE SR02 of the pre-flight Monte Carlo predictions and the post flight BET value shown as vertical lines. For reference, recall that the targets on-board the flight vehicle were generated on L-1 for 8 am launch, although the flight actually flew closer to noon. So the pre-flight Monte Carlo prediction presented here is for a 8 am launch time.

The boosters in ASPIRE SR02 over-performed and led to a higher separation altitude and velocity than the nominal prediction, leading to a trajectory that lofted more than expected. The apogee altitude was 96th percentile of the pre-flight expected distribution (see Fig. 12(a)). Looking at the trajectory states at events through mortar fire, the flight mechanic simulation's pre-flight predictions underestimate the reconstructed BET conditions like Mach number, dynamic pressure, and altitude.

Comparing predictions with the BET at full inflation and splashdown events, as shown in Fig. 13, continues to show that the pre-flight prediction under predicted atmospheric-based conditions like Mach number and dynamic pressure, although other reconstructed states like pull angle between the vehicle and parachute or the splashdown time seem to be within the bounds of the pre-flight predictions.

A similar process to ASPIRE SR01's reconciliation was followed for SR02. Since SR02 had a higher than expected separation altitude and the atmosphere used in the flight software was for 8 am instead of the launch time of 12 pm, it was expected that adjusting for separation states and atmosphere in the reconciliation Monte Carlo would affect the comparison with reconstructed data. During the post flight analysis process for SR02, it was also discovered that there was a misunderstanding of the altitude convention used in the pre-flight atmospheric forecast. The forecast was provided in geopotential altitude while it was assumed in

v0-180 firings

v90-270 firings

(a) Pitch Thruster Firings

(b) Yaw Thruster Firings

vcw-ccw firings

Super firings

(c) Roll Thruster Firings
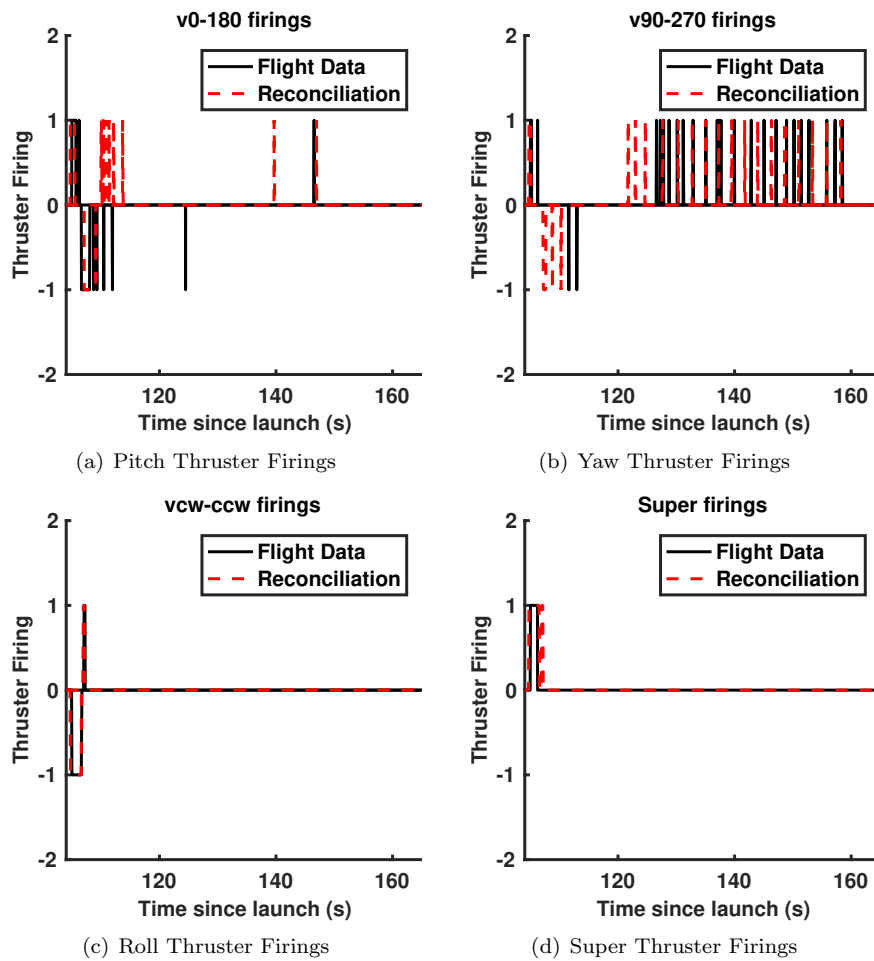
(d) Super Thruster Firings

Figure 9. NIACS firing history reconciliation results for ASPIRE SR01.

the simulation as geodetic altitude. This mistake leads to a difference of a few meters at the altitude of mortar fire. Between the altitude convention change and the time of day's effect on atmospheric parameters, the large difference seen in atmospheric-based states were resolved between the reconstructed values and the reconciled states, as seen in Fig. 14. Recall that the inflation time model was adjusted after SR01 based on that flight's data. That model seems to perform well in SR02 (Fig. 14(d)).

Once adjustments were made to the atmospheric predictions and separation states, the nominal case for the final reconciliation Monte Carlo compares well with the NIACS flight command history recorded on-board as seen in Fig. 15. Once again, although the thruster firings are not identical between the two sets of data, largely the firing histories line up in time. Table 2 shows the integrated NIACS firing time which also show a decent comparison between the flight data and simulation.

Similar to SR01, a small subset of the trajectory states from the reconciliation Monte Carlo nominal are co-plotted with the BET profile in Fig. 16. Once again, the focus here is during the experiment part of the flight, which includes the coast phase and the parachute deployment phase (100 s to 200 s after launch). Although SR02 was not as close to nominal pre-flight prediction as SR01 due to differences in the atmosphere and separation states, one can see that once atmosphere and separation states are adjusted in the simulation to match the day of flight data, the reconciliation simulation is comparable to the BET states.

The ground tracks for SR02 are compared in Fig. 17, where once again the pre-flight prediction used for recovery and the reconciliation Monte Carlo nominal are co-plotted with the BET profile. Unlike SR01, the comparison between BET and the simulation profiles are not as close due to difference in atmosphere and separation states as discussed earlier. Even when the simulation uses the reconstructed atmosphere and uses the actual separation state of the vehicle, the reconciliation comes only with 2 nautical miles. Since the

American Institute of Aeronautics and Astronautics

Table 2. NIACS Integrated Firing Timing for ASPIRE SR02.

Thruster Name	Flight Data (s)	Reconciliation (s)
v0	0.560	1.220
v90	1.360	1.500
v180	0.500	1.050
v270	1.020	1.260
vcw	0.000	0.200
vccw	2.040	2.300
vsuper	0.000	0.000

reconstructed atmosphere is based on balloon data not an on-board sensor, there may be other differences between the simulation and flight, such as lingering atmospheric differences, that do not allow for a closer match.

C. Model Changes from SR01 and SR02

Overall, once simulations were adjusted for conditions not known apriori - such as the actual atmospheric condition during flight or the actual separation state of the ASPIRE payload from the booster - the predictions from the simulations matched the reconstructed states. Thus, there were very few model change recommendations for future flights coming from the analysis of the data from SR01 and SR02. There were few reasons to suggest any changes in the aerodynamics of the payload or the parachute based on the flight data. The NIACS models in the simulation also performed close to the flight data recorded in SR01 and SR02. Small model changes, such as narrowing the dispersion of the inflation time parameters, which was done after SR01 were justified by the results of SR02. However, there is room for procedural changes, such as fixing the altitude conversion misinterpretation or adding targets and predictions for multiple launch times. These changes are planned and they could mitigate the mismatch in atmospheric conditions between the pre-flight simulation and actual flight as was observed in SR02.

V. Conclusions

ASPIRE is a series of sounding rocket tests that aims to answer questions about supersonic parachute inflation and dynamics that were raised by the parachute failures of the predecessor LDSD program. In October 2017, ASPIRE SR01 tested the MSL-heritage DGB parachute and deployed the decelerator near conditions seen by the MSL mission on Mars in 2012. In March 2018, ASPIRE SR02 successfully tested a new strengthened DGB parachute at a dynamic pressure that was fifty percent higher that what was seen for MSL. A multi-body flight dynamics simulation was developed to provide pre-flight vehicle performance predictions and was used to target Mars relevant parachute deployment conditions. The simulation incorporated various engineering models, such as 6DOF test vehicle aerodynamics, 6DOF parachute aerodynamics, NIACS attitude control system models, and atmospheric prediction models. For ASPIRE SR01, based on comparison to early post flight reconstruction results, there was good agreement between the pre-flight predictions and the BET. ASPIRE SR02 saw reconstructed conditions that were lower probability events in the pre-flight predictions, especially for target dynamic pressure values; however, after adjusting for atmospheric and separation state differences, the simulation provided a good match to the reconstructed values. ASPIRE reconstruction and reconciliation process has yielded verification of the pre-flight simulation and adjustments to key models to match flight data and bolsters the simulation to provide improved predictions for future flights.

Acknowledgments

and David Way. Parts of this research were carried out at the Jet Propulsion Laboratory, California Institute of Technology, under a contract with the National Aeronautics and Space Administration.

References

[1] Tanner, C., Clark, I., and Chen, A., "Overview of the Mars 2020 Parachute Risk Reduction Plan," IEEE Paper No. *IEEE Aerospace Conference 2018,* Big Sky, MT, 2018.

[2] Cruz, J. R., Way, D. W., Shidner, J. D., Davis, J., Adams, D. S., and Kipp, D., "Reconstruction of the Mars Science Laboratory Parachute Performance," *Journal of Spacecraft and Rockets*, Vol. 51, No. 4, 2014, pp. 1185–1196.

[3] Ivanov, M. and Tibbets, B., "Low Density Supersonic Decelerator Flight Dynamics Test - 1 Flight Design and Targeting," AIAA 2015-2152*, AIAA Aerodynamic Decelerator Systems Conference,* Daytona Beach, FL, 2015.

[4] Strauss, W., "Construction of Supersonic Flight Dynamics Test Vehicle Monte Carlo Splashdown Footprints for use in Range Safety and Recovery Operations," AAS 16-288, *AAS/AIAA Space Flight Mechanics Conference,* Napa, CA, 2016.

[5] Braun, R. D., Powell, R. W., Engelund, W. C., Gnoffo, P. A., Weilmuenster, K. J., and Mitcheltree, R. A., "Mars Pathfinder Six-Degree-of-Freedom Entry Analysis," *Journal of Spacecraft and Rockets*, Vol. 32, No. 6, 1995, pp. 993–1000.

[6] Desai, P. N., Schoenenberger, M., and Cheatwood, F. M., "Mars Exploration Rover Six-Degree-of-Freedom Entry Trajectory Analysis," *Journal of Spacecraft and Rockets*, Vol. 43, No. 5, Sept. 2006, pp. 1019–1025.

[7] Desai, P. N., Prince, J. L., Queen, E. M., Schoenenberger, M., Cruz, J. R., and Grover, M. R., "Entry, Descent, and Landing Performance of the Mars Phoenix Lander," *Journal of Spacecraft and Rockets*, Vol. 48, No. 5, 2011, pp. 798–808.

[8] Way, D. W., Davis, Jody, D., and Shidner, J. D., "Assessment of the Mars Science Laboratory Entry, Descent, and Landing Simulation," AAS 13-420*, AAS/AIAA Space Flight Mechanics Conference, Kauai, HI*, 2013.

[9] Bowes, A., Davis, J. D., Dutta, S., Striepe, S., Ivanov, M., Powell, R., and White, J. P., "LDSD POST2 Simulation and SFDT-1 Pre-flight Launch Operations Analyses," AAS 15-232, *AAS/AIAA Space Flight Mechanics Conference,* Williamburg, VA, 2015.

[10] White, J., Dutta, S., and Striepe, S., "SFDT-1 Camera Pointing and Sun-Exposure POST2 Analysis and Flight Performance," AAS 15-218, *AAS/AIAA Space Flight Mechanics Conference,* Williamburg, VA, 2015.

[11] Dutta, S., Bowes, A., Striepe, S., Davis, J. D., Blood, E. M., and Ivanov, M., "Supersonic Flight Dynamics Test 1 - Postflight Assessment of Simulation Performance," AAS 15-219, *AAS/AIAA Space Flight Mechanics Conference,* Williamsburg, VA, 2015.

[12] White, J. P., Bowes, A., Dutta, S., Ivanov, M., and Queen, E., "LDSD POST2 Modeling Enhancements in Support of SFDT-2 Flight Operations," AAS 16-221, *AAS/AIAA Space Flight Mechanics Conference,* Napa, CA, 2016.

[13] Dutta, S., Bowes, A., White, J., Striepe, S., Queen, E., O'Farrell, C., and Ivanov, M., "Post-Flight Assessment of Low Density Supersonic Decelator Flight Dynamics Test 2 Simulation," AAS 16-222, *AAS/AIAA Space Flight Mechanics Conference,* Napa, CA, 2016.

[14] Leslie, F. and Justus, C., "The NASA Marshall Space Flight Center Earth Global Reference Atmosphere Model - 2010 Version," Tech. rep., NASA/TM-2011-216467, 2011.

[15] Molod, A., Takacs, L., Suarez, M., Bacmeister, J., Song, I., and Eichmann, A., "The GEOS-5 Atmospheric General Circulation Model: Mean Climate and Development from MERRA to Fortuna," Tech. Rep. NASA TM 2012-104606-VOL-28, NASA GFSC, 2012.

[16] Toniolo, M., Tartabini, P., Pamadi, B., and Hotchko, N., "Constraint Force Equation Methodology for Modeling Multi-Body Stage Separation Dynamics," AIAA 2008-219, *AIAA Aerospace Sciences Meeting and Exhibit,* Reno, NV, 2008.

[17] Van Norman, J., "ASPIRE Payload Aerodynamic Models and Reconstruction," AIAA Paper No. *AIAA SciTech 2019,* San Diego, CA, 2019.

[18] Muppidi, S., OFarrell, C., Tanner, C., Van Norman, J., and Clark, I., "Modeling and Flight Performance of Supersonic Disk-Gap-Band Parachutes In Slender Body Wakes," AIAA Paper No. *AIAA AVIATION 2018,* Atlanta, GA, 2018.

[19] O'Farrell, C., Karlgaard, C., Dutta, S., Queen, E., Ivanov, M., and Clark, I., "Overview and Reconstruction of the ASPIRE Project's SR01 Supersonic Parachute Test," IEEE Paper No. *IEEE Aerospace Conference,* Big Sky, MT, 2018.

[20] Cruz, J., Way, D., Shidner, J., Davis, J., Powell, R., Kipp, D., Adams, D., Sengupta, A., Witkowski, A., and Kandis, M., "Parachute Models Used in the Mars Science Laboratory Entry, Descent, and Landing Simulation," AIAA 2013-1276, *AIAA Aerodynamic Decelerator Systems (ADS) Conference,* Daytona Beach, FL, 2013.

[21] Greene, G., "Opening Distance of a Parachute," *Journal of Spacecraft*, Vol. 7, No. 1, 1970, pp. 98–100.

[22] Way, D., "A Momentum-Based Indicator for Predicting the Peak Opening Load of Supersonic Parachutes," IEEE Paper No. *IEEE Aerospace Conference,* Big Sky, MT, 2018.

[23] Karlgaard, C., Tynis, J., and O'Farrell, C., "Reconstruction of the Advanced Supersonic Parachute Inflation Research Experiment (ASPIRE) Sounding Rocket Flight Test," AIAA Paper No. *AIAA Atmospheric Flight Mechanics Conference,* Atlanta, GA, 2018.
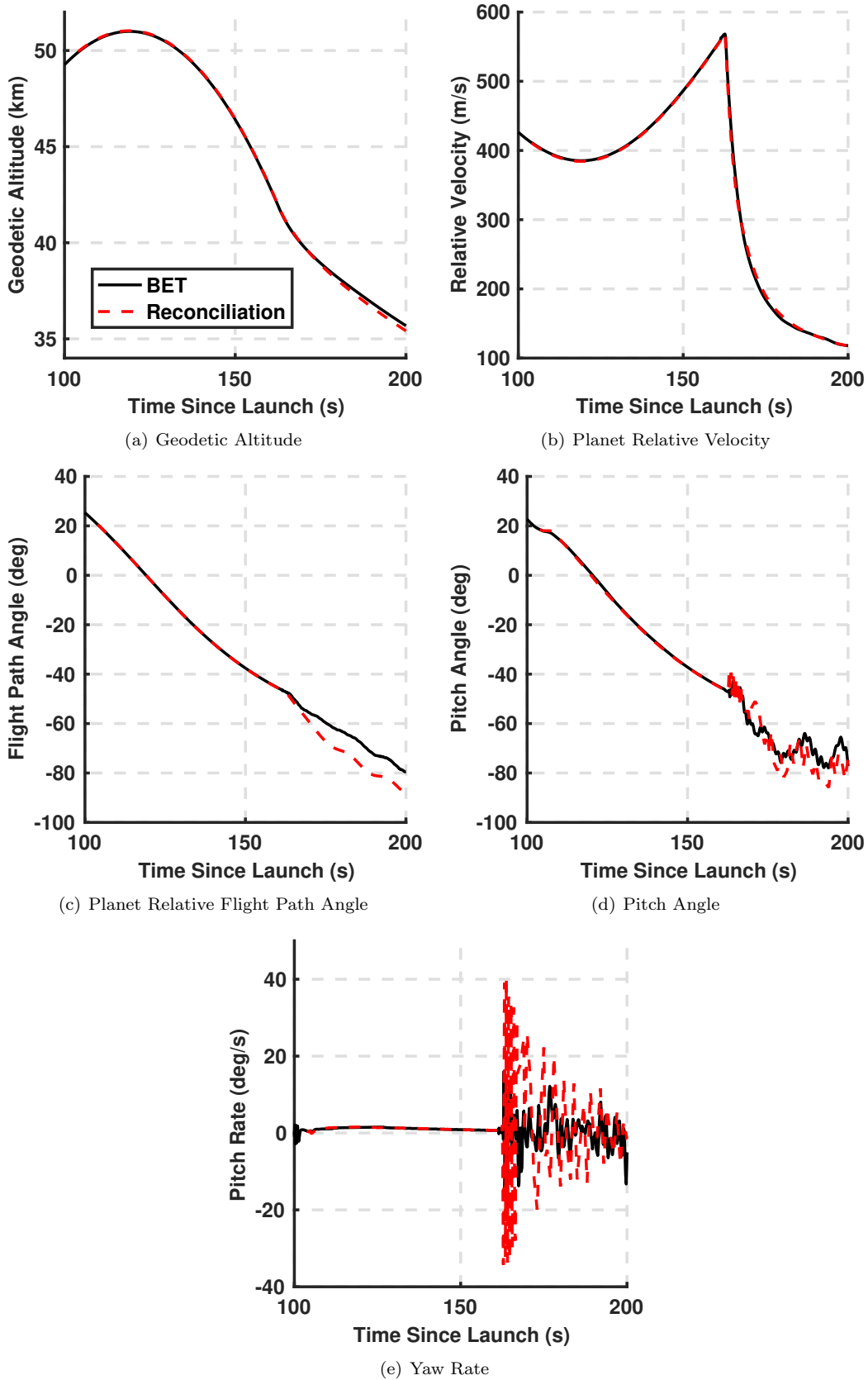
(a) Geodetic Altitude

(b) Planet Relative Velocity

(c) Planet Relative Flight Path Angle

(d) Pitch Angle

(e) Yaw Rate

Figure 10. Trajectory comparison between BET and simulation for ASPIRE SR01.

(a) Trajectory   (b) Splashdown Location   (c)
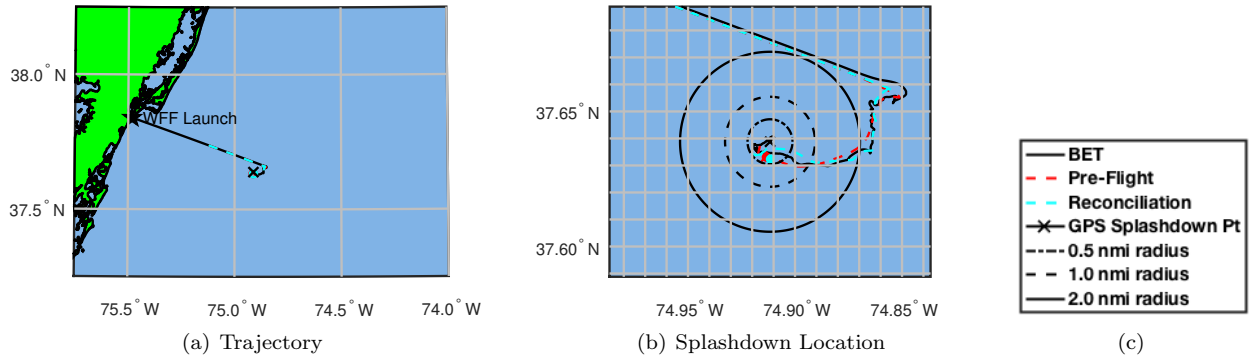
Figure 11. Ground track comparison between BET and simulation for ASPIRE SR01.

(a) Apoapsis Altitude   (b) Mach at Mortar Fire

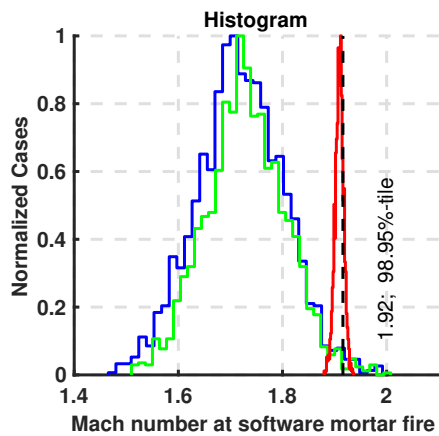(c) Dynamic Pressure at Mortar Fire   (d) Total Angle of Attack at Mortar Fire
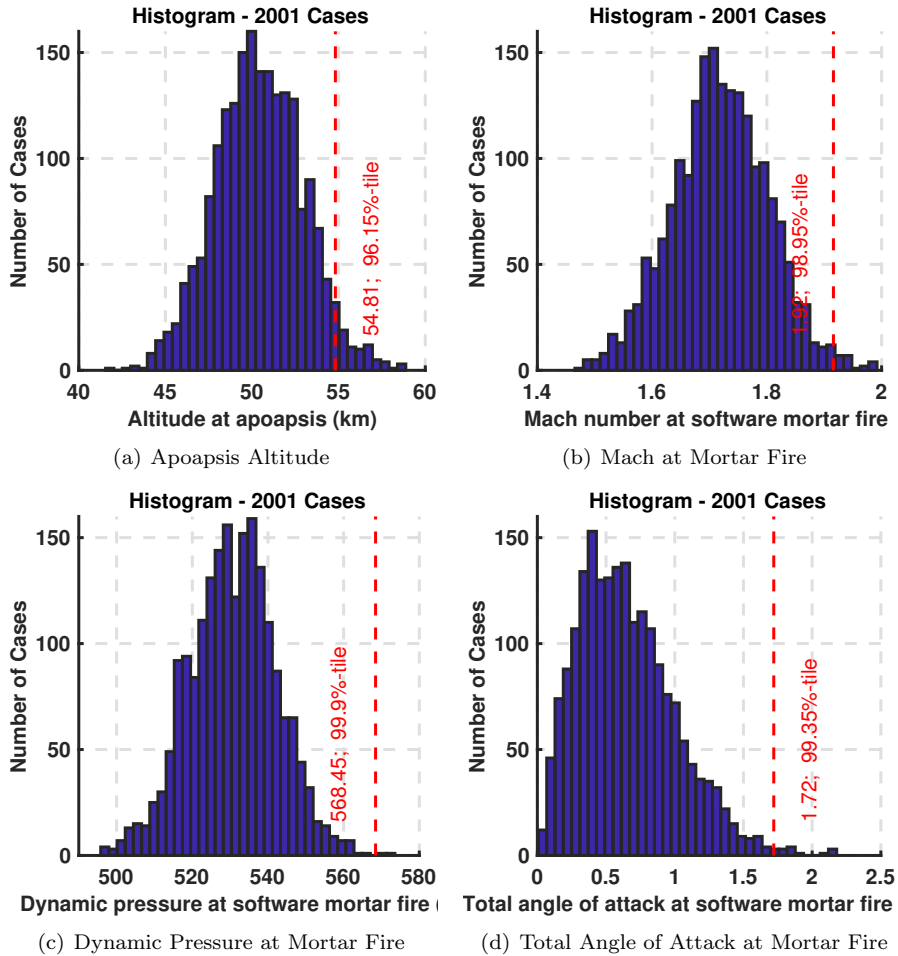
Figure 12. Pre-flight Monte Carlo predictions (histograms) and comparison to reconstruction (red line) through mortar fire for ASPIRE SR02. Pre-flight Monte Carlo predictions are for a 8 am flight.

American Institute of Aeronautics and Astronautics

(a) Mach at Full Inflation

(b) Dynamic Pressure at Full Inflation

(c) Pull Angle at Full Inflation

(d) Time at Splashdown
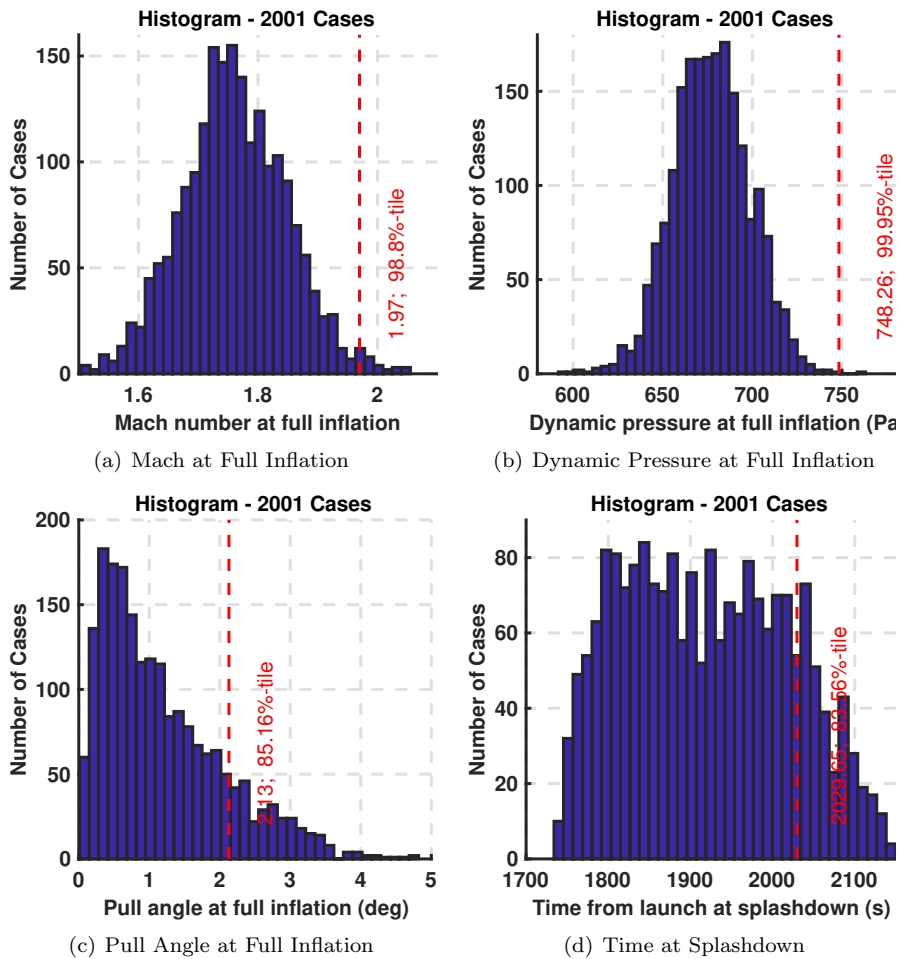
Figure 13. Pre-flight Monte Carlo Predictions (histograms) and comparison to Reconstruction (red line) through Splashdown for ASPIRE SR02. Pre-flight Monte Carlo predictions are for a 8 am flight.
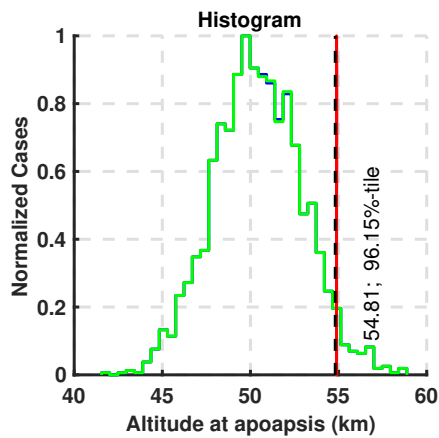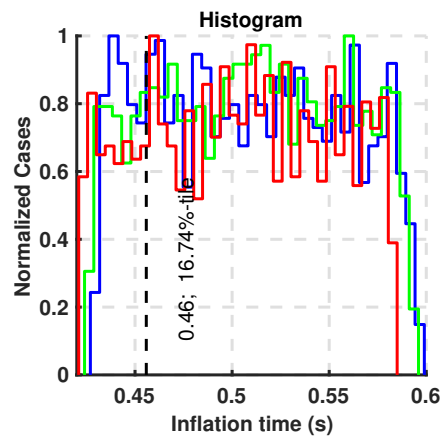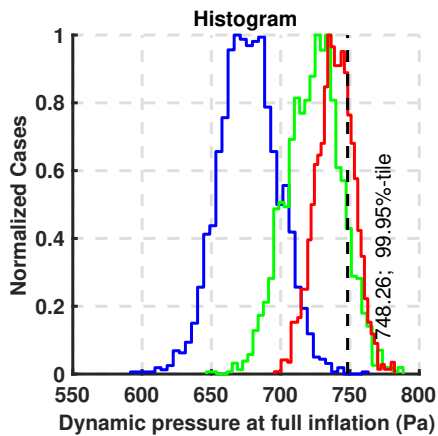
(a) Altitude at Apoapsis
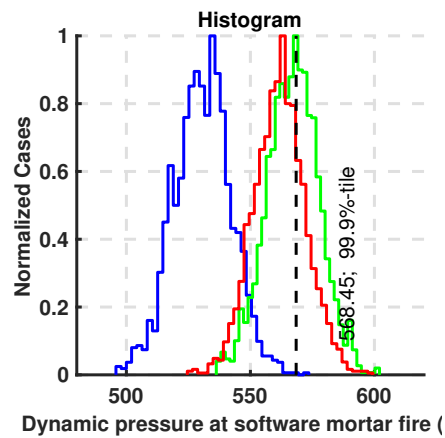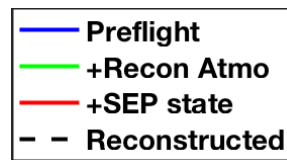
(b) Dynamic Pressure at Software Mortar Fire

(c) Mach at Software Mortar Fire

(d) Inflation Time

(e) Dynamic Pressure at Full Inflation

(f)

Figure 14. Reconciliation results for ASPIRE SR02. Reconstruction line in black shows the percentile compared to the pre-flight 8 am prediction.
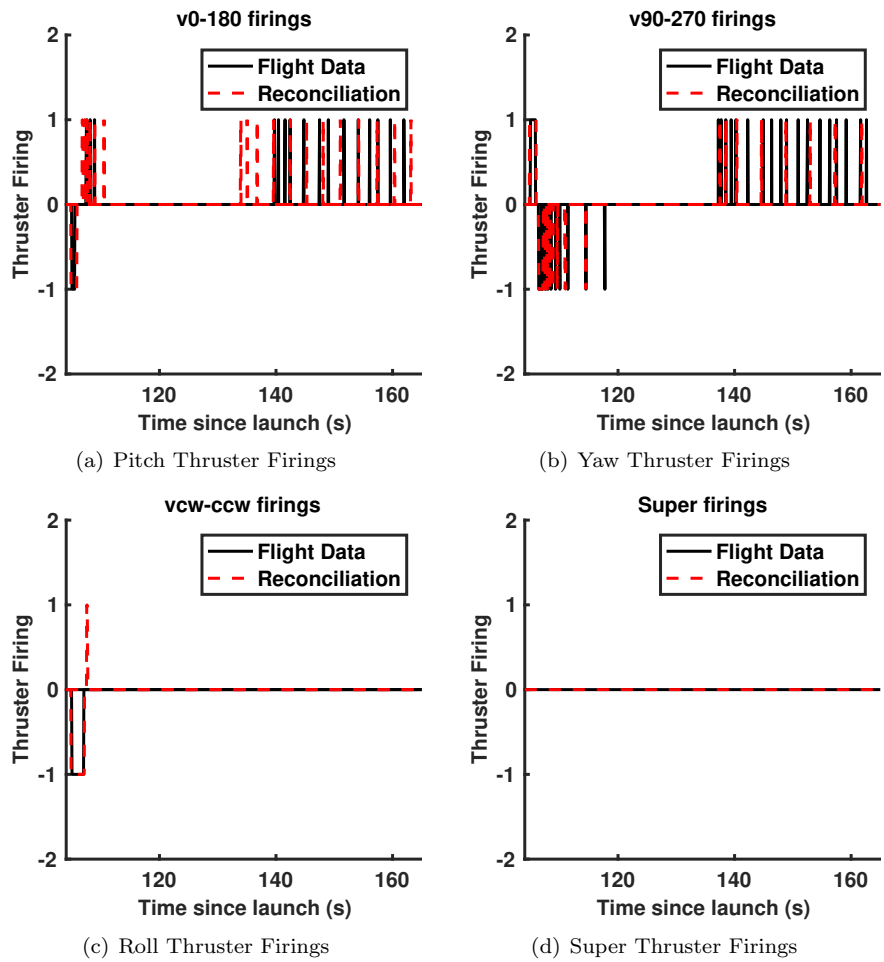
(a) Pitch Thruster Firings

(b) Yaw Thruster Firings

(c) Roll Thruster Firings

(d) Super Thruster Firings

Figure 15. NIACS firing history reconciliation results for ASPIRE SR02.

(a) Geodetic Altitude

(b) Planet Relative Velocity

(c) Planet Relative Flight Path Angle

(d) Pitch Angle

(e) Yaw Rate
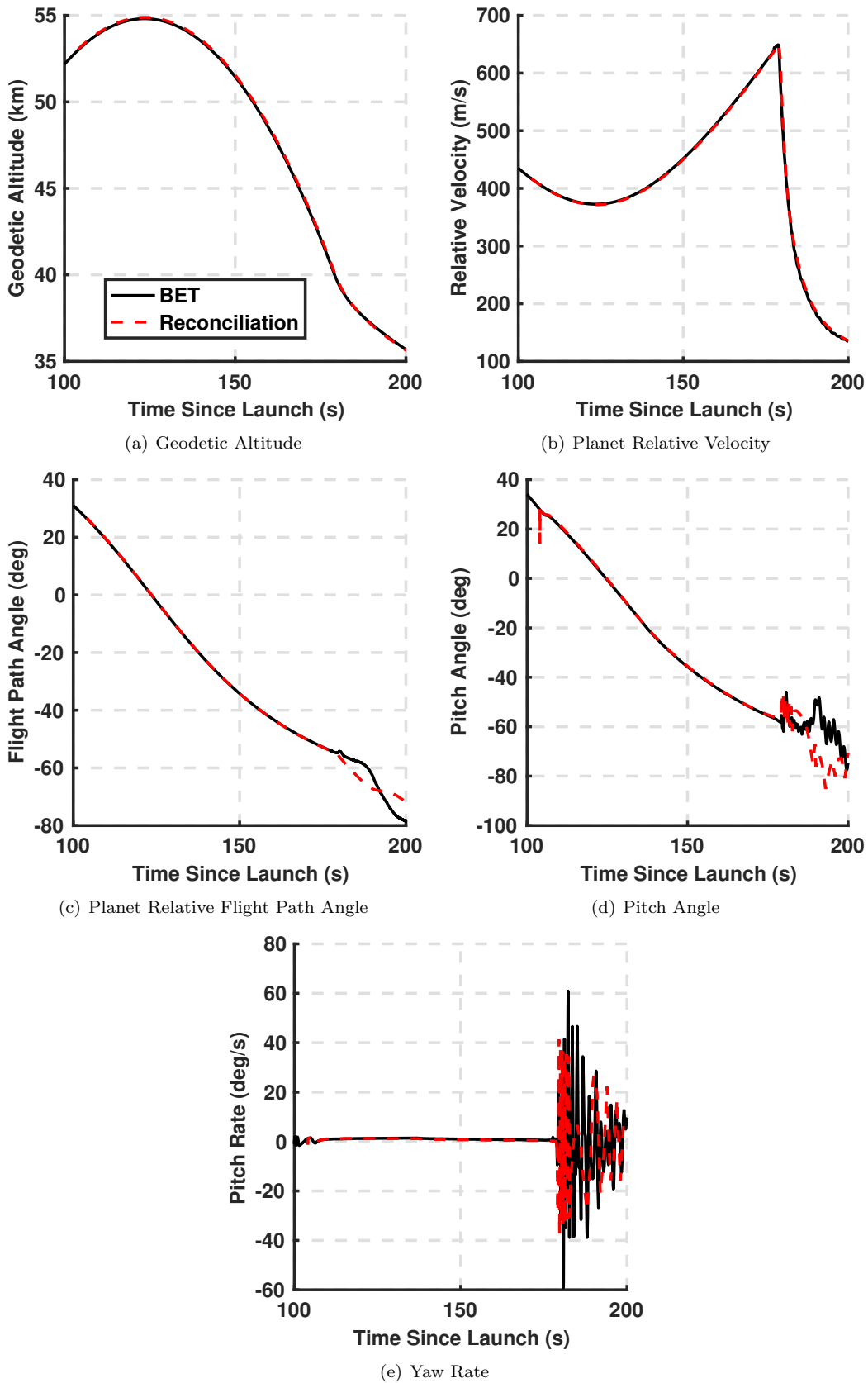
Figure 16. Trajectory comparison between BET and simulation for ASPIRE SR02.

American Institute of Aeronautics and Astronautics

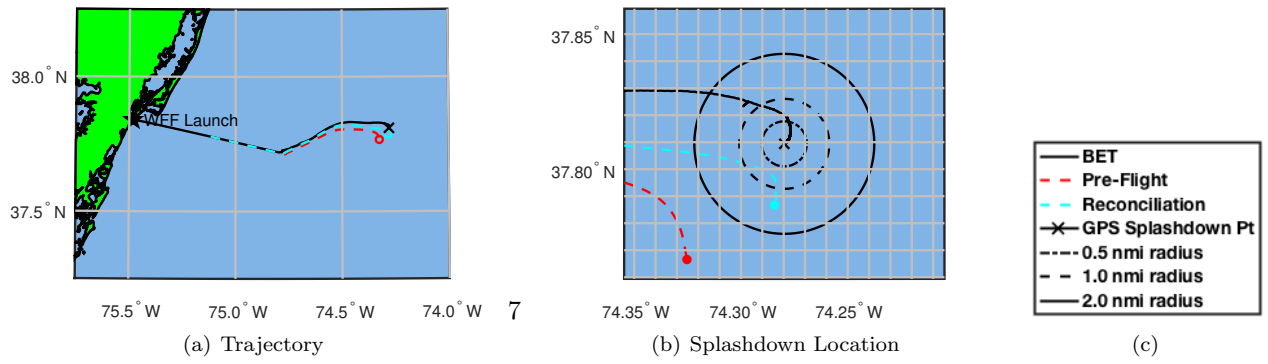(a) Trajectory

(b) Splashdown Location

(c)

Figure 17. Ground track comparison between BET and simulation for ASPIRE SR02.

American Institute of Aeronautics and Astronautics